Mechanistic Inquiry into the Role of Tissue Remodeling in Fibrotic Lesions in Human Atrial Fibrillation

Kathleen S. McDowell,[†] Fijoy Vadakkumpadan,[†] Robert Blake,[†] Joshua Blauer,[‡] Gernot Plank,[§] Rob S. MacLeod,[‡] and Natalia A. Trayanova[†*]

[†]The Johns Hopkins University, Department of Biomedical Engineering and Institute for Computational Medicine, Baltimore, Maryland; [‡]University of Utah, Comprehensive Arrhythmia Research and Management Center, School of Medicine, Salt Lake City, Utah; and [§]Medical University of Graz, Institute of Biophysics, Graz, Austria

ABSTRACT Atrial fibrillation (AF), the most common arrhythmia in humans, is initiated when triggered activity from the pulmonary veins propagates into atrial tissue and degrades into reentrant activity. Although experimental and clinical findings show a correlation between atrial fibrosis and AF, the causal relationship between the two remains elusive. This study used an array of 3D computational models with different representations of fibrosis based on a patient-specific atrial geometry with accurate fibrotic distribution to determine the mechanisms by which fibrosis underlies the degradation of a pulmonary vein ectopic beat into AF. Fibrotic lesions in models were represented with combinations of: gap junction remodeling; collagen deposition; and myofibroblast proliferation with electrotonic or paracrine effects on neighboring myocytes. The study found that the occurrence of gap junction remodeling and the subsequent conduction slowing in the fibrotic lesions was a necessary but not sufficient condition for AF development, whereas myofibroblast proliferation and the subsequent electrophysiological effect on neighboring myocytes within the fibrotic lesions was the sufficient condition necessary for reentry formation. Collagen did not alter the arrhythmogenic outcome resulting from the other fibrosis components. Reentrant circuits formed throughout the noncontiguous fibrotic lesions, without anchoring to a specific fibrotic lesion.

INTRODUCTION

Atrial fibrillation (AF) is the most common cardiac arrhythmia associated with patient morbidity and mortality, affecting over two million people in the United States alone (1). AF is initiated when triggered activity from the pulmonary veins (PVs) propagates into atrial tissue and, via mechanisms incompletely understood, degrades into reentrant activity (2). Catheter ablation, including the electrical isolation of PVs to prevent ectopic signal propagation into atrial chambers, has emerged as a promising treatment strategy for patients who suffer from AF. However, overall success rates for terminating AF via catheter ablation are low, with recent surveys reporting only 70% success (3). Advancements in catheter ablation procedures are hindered by the elusive nature of the mechanisms underlying AF.

Recent clinical and experimental studies have convincingly demonstrated a correlation between atrial fibrosis and AF. Atrial biopsies from paroxysmal AF patients show increased interstitial fibrosis compared to sinus rhythm control subjects (4). Studies of explanted human hearts demonstrate that atrial collagen volume correlates positively with AF persistence when comparing nonarrhythmic individuals to those who suffer permanent and persistent AF (5). Furthermore, atrial fibrosis has been documented in patients who develop postoperative AF (6). In a study in which late gadolinium-enhanced magnetic resonance imaging (LGE-MRI) was used before ablation to quantify the extent of fibrosis in the left atrial (LA) wall, it was found that an increased amount of LA fibrosis is strongly associated with AF recurrence after catheter ablation (7). Although these findings convincingly show a correlation between atrial fibrosis and AF, the causal relationship between fibrosis and AF remains incompletely understood.

Fibrotic remodeling of atrial tissue involves processes that occur in parallel across multiple scales. Gap junction remodeling (GJR) at the membrane level (8), fibroblast phenotype switching at the cellular level (9), and the deposition of excess collagen at the tissue level (5) give rise to complex interactions at the organ level, setting the stage for AF initiation in the fibrotic atria. In addition, studies also indicate that the extent and distribution of fibrotic lesions within the human LA, the quantification of which has recently been made possible by improved MRI technology, may also contribute mechanistically to AF susceptibility (10). Given the complex and interdependent nature of the remodeling processes involved in fibrosis, compounded by its heterogeneous distribution throughout the human atrium, isolating the unique mechanisms by which fibrosis and its components contribute to human AF is difficult to achieve experimentally. However, the ability to obtain high-resolution images in vivo that capture both patient atrial geometry and fibrotic distribution makes it possible to reconstruct patient-specific LA geometries with accurate fibrotic lesion morphology (11). A computational model with accurate representation of atrial geometry and fibrotic lesion distribution presents a powerful tool to explore how fibrotic remodeling

Submitted March 8, 2013, and accepted for publication May 10, 2013.

*Correspondence: ntrayanova@jhu.edu

Editor: Andrew McCulloch.

0006-3495/13/06/2764/10 $2.00

http://dx.doi.org/10.1016/j.bpj.2013.05.025

at the membrane, cellular, and tissue-level give rise to an arrhythmogenic substrate at the organ level.

The goal of this study was to determine the mechanisms by which fibrosis in the human atria underlies the degradation of a PV ectopic beat into AF. To achieve this goal, we used a realistic model of atrial fibrosis distribution generated from high-resolution LGE-MRI images acquired in vivo from a patient suffering from persistent AF. Modeling the fibrotic lesions incorporated representations of collagen deposition, GJR, and myofibroblast proliferation. Simulations with eight different atrial fibrosis models developed from the baseline LA geometric model were performed to determine how each component of fibrotic remodeling as well as their combinations contributes to the arrhythmogenic substrate.

METHODS

Detailed Methods are available in the online Supporting Material. Briefly, a patient with persistent AF presenting for catheter ablation underwent LGE-MRI acquisition (12); a representative slice of the MR image stack is shown in Fig. 1. Image segmentation and interpolation resulted in a high-resolution image of the atrial wall with extensive fibrotic lesions (Fig. 1); the fibrotic lesion size and distribution in this patient was typical for patients with extensive fibrosis in the LA and persistent AF (12). We chose to model only the LA based on the fact that 94% of ectopic beats that result in AF initiation originate in the PVs (2) and 76% of AF sources (among which electrical rotors) were found to be located in the LA (13). A finite element

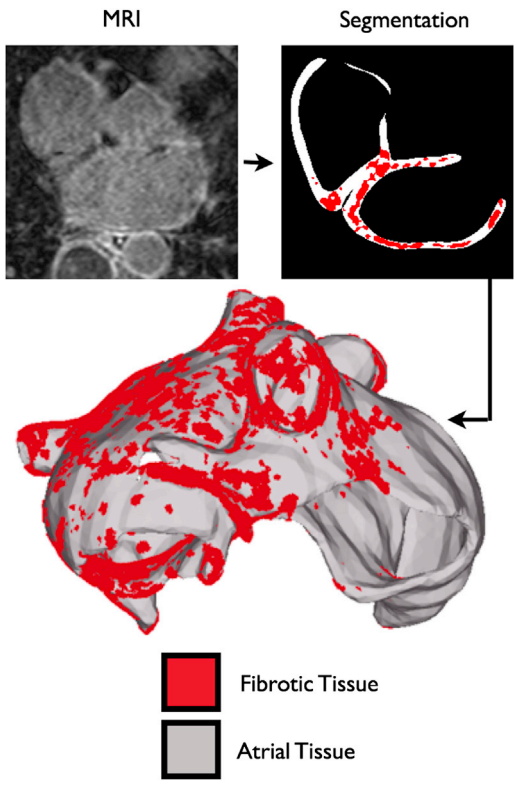

FIGURE 1 Model generation. Representative MRI slice of the human heart, segmentation of the atrial tissue, and construction of the 3D atrial model.

tetrahedral mesh was generated from the segmented image stack, and fiber orientation was incorporated as previously described (11,14) (see the Supporting Material). Nonfibrotic regions of the tissue were represented with a modified version of the Courtemanche et al. (15) model of the human atrial action potential under AF conditions, as described by Krummen et al. (16); the model also included the formulation of the acetylcholine-activated potassium current, $I_{K(ACh)}$, from Kneller et al. (17) Conductivities were chosen such that conduction velocity fell within the range recorded in the human atrium (18); additional details can be found in the Supporting Material.

Modeling fibrotic tissue

Atrial fibrosis is characterized by numerous pathophysiological processes: 1), a progressive thickening of the interstitial matrix, including diffuse collagen deposition and subsequent separation of individual myocytes; 2), GJR due to connexin 43 (Cx43) protein downregulation and lateralization; and 3), fibroblast proliferation and phenotype switching into myofibroblasts. Although these aspects of remodeling progress simultaneously, it is useful to separate the different fibrotic manifestations to isolate and investigate their unique contributions to the arrhythmogenic substrate. For this reason, eight distinct atrial models were generated for the study, based on the original atrial geometry and fibrotic lesion distribution, but each with a unique representation of one or more components of fibrosis (see Table 1, *left column*). One control model was constructed, in which no fibrotic structural remodeling was included in the atrium (i.e., the fibrotic lesions were assumed to have the properties of nonfibrotic atrial myocardium). Three models, each with one of the previous components of fibrosis (diffuse collagen deposition, GJR, or myofibroblast proliferation with coupling to myocytes) in the fibrotic lesions were developed. Additionally, three models, each with a combination of two of the previous components in the fibrotic lesions, were generated. Finally, one model that included all three of the previous characteristics in the fibrotic lesions was constructed. Detailed descriptions of the model representations of each of the three components of fibrosis are found below. All fibrotic remodeling was confined to the patient-specific fibrotic lesions, i.e., the red regions in Fig. 1.

Under AF (5), collagen deposition in the LA is upregulated and typically presents diffuse architecture (i.e., is parallel to muscle bundles). To represent this diffuse collagen deposition in the fibrotic lesions, we employed a method of 3D decoupling of the finite elements in the model that correspond to fibrotic lesions, as described in the Supporting Material, thus simulating the fine conduction barriers introduced by collagen along the fiber direction. This method was first developed in 2D by Costa el al. (19), and we have recently extended the technique to 3D (11). Additional simulations were performed to test the implications of patchy collagen (i.e., collagen that is both parallel and transverse to muscle bundles), because evidence exists suggesting that this architecture may also be present in the fibrotic atrium in AF (20). Patchy collagen was represented as passive insulators interrupting both transverse and longitudinal connections between cells, as

TABLE 1 Outcome of PV ectopy in the LA models with different components of fibrosis

	Occurrence of block	Reentry
Control	O	O
GJR	✓	O
Collagen deposition (patchy or diffuse)	O	O
Myofibroblast coupling	O	O
GJR & collagen deposition (patchy or diffuse)	✓	O
Collagenous deposition (patchy or diffuse) & myofibroblast coupling	O	O
GJR & myofibroblast coupling	✓	✓
GRJ, collagenous deposition (patchy or diffuse), & myofibroblast coupling	✓	✓

done in previous computational studies (21–23). Two densities of this patchy collagen deposition, 1% and 10% collagen by volume were randomly distributed throughout the fibrotic regions. These densities were based on experimental data for the human LA under AF, where up to 7% collagen by volume was documented, when considering both collagen types I and III (5).

A study examining atrial substrates in patients with AF found that the more collagen deposited in each substrate, the less Cx43 expressed (24); the overall reduction of Cx43 volume fraction observed in atria in chronic AF compared to sinus rhythm was found to be ~30%. Likewise, atrial biopsies from human patients with AF exhibited Cx43 lateralization (8) rather than localization at the intercalated discs; lateral Cx43 labeling (as a percentage of the total amount of Cx43 per myocyte) was found to be 3.9-fold higher in atrial free wall myocytes in the AF group compared to sinus rhythm. To represent this GJR, myocardial conductivity values in the fibrotic lesions of the model were decreased by 53% in the longitudinal direction and increased by 2.5-fold in the transverse direction, compared to the nonfibrotic conductivities in the remainder of the atria (11), thus achieving a 30% reduction in combined conductivity (as measured by Cx protein expression quantification methods) and a 3.9-fold increase in the ratio of transverse/combined conductivity.

Finally, myofibroblast properties were randomly assigned to 1% of the fibrotic lesions to represent the myofibroblast proliferation observed experimentally under fibrosis conditions (25). Myofibroblasts were electrically connected to adjacent myocytes, as observed experimentally (26), and membrane kinetics was modeled following our previously published methodology (11,27).

Simulation protocol and data analysis

Mathematical description of current flow was based on the monodomain representation of the myocardium and simulations were executed using the simulation package CARP (CardioSolv LLC) (28). To test the arrhythmogenic propensity of the atrial models with different fibrotic representations, each substrate was paced for 5 beats at 365 ms cycle length, followed by two premature beats (S2 and S3) at cycle lengths ranging from 230 to 260 ms. Preliminary studies identified this pacing sequence as the most computationally efficient protocol to initiate AF; extending the stimulus protocol did not alter arrhythmia outcomes. Stimulus location was also chosen after preliminary results indicated that pacing from various locations in the PVs resulted in the formation of identical AF rotors, indicating that the substrate (and not pacing location) determined rotor location. Therefore, a single stimulus site was used for this study, located between the left superior and inferior PVs (Fig. 2, *red dot*, at *top left*). The initiation of reentrant arrhythmia was defined as the occurrence of unidirectional block and subsequent formation of a reentrant circuit following the premature beats. The formation of a reentrant circuit was assumed to mark the initiation of AF due to recent evidence that localized rotors or focal impulses are detected in 97% of patients with sustained AF (13).

To delineate how the various components of fibrosis differentially contribute to arrhythmia propensity in the fibrotic atria, each substrate was analyzed in several ways:

1. To assess the influence of the fibrotic components on conduction, activation maps were constructed for each atrial model. Activation time was considered to be the time between S2 stimulus and local time of excitation, defined as the time at which transmembrane potential exceeded a threshold of −20 mV.
2. Myofibroblasts have a less negative resting membrane potential (V_{REST}) than myocytes, and thus can cause diastolic depolarization in myocytes with which they electrically couple. Indeed, research has shown that cardiomyocytes exhibit a myofibroblast density-dependent gradual depolarization when coated with myofibroblasts (29). Thus, maps of V_{REST} were generated for each atrial model to characterize the spatial distribution of diastolic potential and analyze its effect on conduction.
3. Experimental evidence suggests that myofibroblasts can alter the action potential duration (APD) of myocytes with which they electrically couple (30). At the tissue level, APD dispersion can increase the susceptibility of the substrate to arrhythmia (31). Therefore, APD maps for each atrial model were generated by calculating the local durations from peak action potential amplitude to 90% repolarization.

RESULTS

Effects of atrial fibrosis on propensity to arrhythmia

Propensity to arrhythmia following premature (ectopic) beats in the PVs was assessed in each of the eight models; events such as occurrence of conduction block and subsequent reentry are summarized in Table 1. Neither unidirectional block nor reentry occurred in the control (i.e., nonfibrotic) case. Conduction block took place in all models that incorporated GJR in the fibrotic regions. The inclusion of diffuse collagen deposition or myofibroblasts (in combination or alone) in the fibrotic regions did not result in conduction block following ectopic wave propagation. However, when either of these components of fibrosis was combined with GJR in the fibrotic lesions, conduction block ensued. Likewise, in the scenario in which all three fibrosis characteristics were modeled, block was observed. Therefore, this study found that the remodeling of gap junctions in fibrotic lesions was the primary contributor to conduction block following PV ectopy in the atrium, and the addition of other components of fibrosis did not suppress the occurrence of conduction block. When collagen of patchy architecture was incorporated at densities of 1% and 10% by volume (instead of diffuse collagen), arrhythmia outcomes were identical to those resulting from diffuse collagen, as presented in Table 1.

The formation of reentry is contingent upon first the occurrence of block, but does not arise in all cases of block. Of the four scenarios in which conduction block occurred (fibrotic lesions modeled with GJR alone; GJR and collagen deposition, GJR and myofibroblasts coupled to myocytes, and GJR with both myofibroblasts and collagen deposition), only the latter two (i.e., models that represented myofibroblasts coupled to myocytes in the fibrotic lesions) resulted in reentry. In both of these cases, the reentrant circuit subsequently degraded into sustained AF that lasted for at least 15 s (the maximum computationally practical time tested). GJR in the fibrotic lesions alone did not support the formation of a reentrant circuit, and the presence of patchy or diffuse collagen had no effect on the substrate's propensity to arrhythmia in any of the models. Thus, our simulation results indicate that the presence of myofibroblasts coupled to myocytes is the critical condition for reentry formation following conduction block in the fibrotic atrium. The addition of other components of fibrotic remodeling did not alter the substrate's ability to form a reentrant circuit.

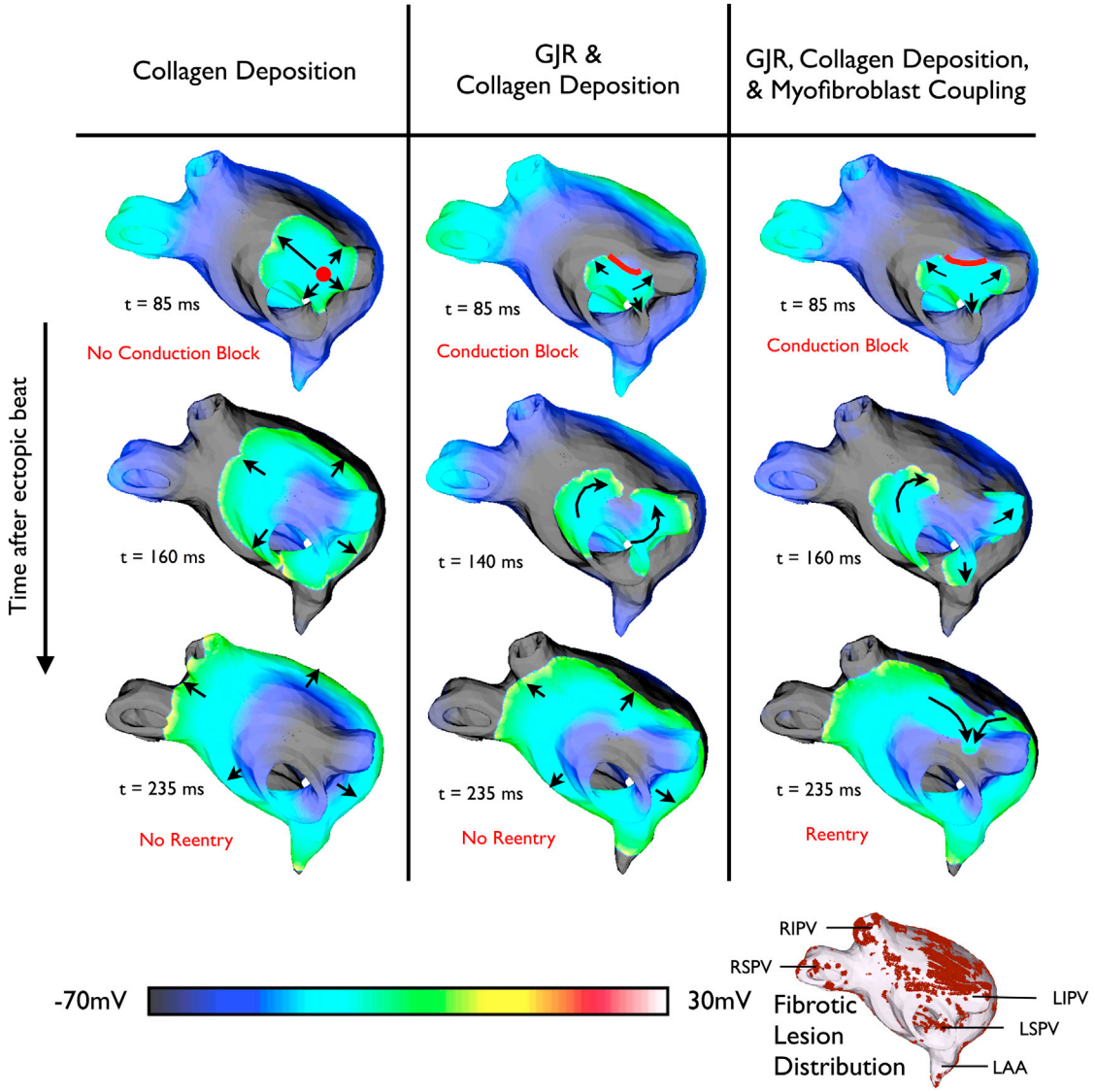

FIGURE 2 Transmembrane potential maps at three time instants in three atrial models with different arrhythmogenic outcomes: neither conduction block takes place nor reentry is established (*leftmost column*; exclusively diffuse collagen deposition modeled in the fibrotic lesions); conduction block occurs without the formation of a reentrant circuit (*middle column*; GJR and diffuse collagen deposition included in the fibrotic lesions), and both conduction block and reentry occur, initiating AF (*rightmost column*; GJR, diffuse collagen deposition, and myofibroblasts coupled to myocytes included in fibrotic lesions). Lines of block are marked in red. Black arrows indicate direction of propagation. Fibrotic distribution is pictured at bottom right, with anatomical labels for the LA appendage (LAA), right superior PV (RSPV), right inferior PV (RIPV), left superior PV (LSPV), and left inferior PV (LIPV).

Fig. 2 presents a summary of the three possible outcomes following a PV ectopic propagation (with conduction pathways shown): neither conduction block nor reentry is established (*leftmost column*; exclusively diffuse collagen deposition is modeled in the fibrotic lesions); conduction block occurs without the formation of a reentrant circuit (*middle column*; GJR and diffuse collagen deposition are included in the fibrotic lesions in the case presented in the figure); and both conduction block and reentry occur to initiate AF (*rightmost column*; GJR, diffuse collagen deposition, and myofibroblasts coupled to myocytes are included in the fibrotic lesions in the model shown). Other combinations of fibrosis components not included in Fig. 2 exhibited conduction patterns similar to those pictured for the corresponding PV ectopy outcome.

Mechanism for conduction block in fibrotic lesions

The electrophysiological properties of substrates that exhibited conduction block following ectopic beats (i.e., atrial models with GJR in fibrotic regions) were compared to those of substrates that were not susceptible to conduction block (i.e., atrial models without GJR in the fibrotic regions). Slowed conduction and discontinuous propagation were observed in all models that experienced conduction

block. To illustrate this finding, activation maps following a premature beat from the left PVs of select substrates are displayed in Fig. 3. Activation times following a premature beat are longer than those in sinus rhythm or following slower pacing rates due to the steep conduction velocity restitution experienced by patients who suffer from AF (32); AF patients show a conduction slowing of ~48% with rate acceleration (33).

In a substrate with only collagen distribution (diffuse or patchy) incorporated into the fibrotic lesions (*left-most substrate* in Fig. 3), conduction propagated in a fairly smooth and continuous manner, as indicated by the uniform and concentric activation pattern. The collagen deposition did not disrupt conduction in the model. This finding is supported by the experimental evidence that collagen of diffuse architecture (as often found in human atria (5,34)) has a minimal effect on conduction delay, even at high densities (35). Furthermore, although patchy collagen architecture at higher densities has been shown to affect conduction in the ventricles (35), existing experimental data do not indicate that the density (up to 7%) (5) of collagen of patchy architecture found in the human LA under AF contributes to conduction abnormalities.

In the substrate that contained only myofibroblasts coupled to myocytes as a representation of fibrosis (*2nd from left substrate* in Fig. 3), conduction through tissue proceeded discontinuously (with jagged isochrones) as it traversed more slowly through fibrotic lesions than through nonfibrotic tissue, although total LA activation time was only 5 ms longer than control. Myofibroblasts were the culprit of this slowing of conduction within fibrotic lesions, because they caused V_{REST} elevation in myocytes with which they were electrically coupled (29), resulting in partial sodium channel inactivation. Indeed, as indicated in Fig. 4 *A*, a myocyte within a fibrotic lesion experienced an elevated V_{REST} of -74.5 mV, compared to V_{REST} of -78mV within a lesion but without myofibroblasts. At the organ level, distribution of V_{REST} elevation in substrates with electrically coupled myofibroblasts (see Fig. 4 *C*, *bottom row*) followed the pattern of fibrotic lesion distribution (*as pictured* in Fig. 2). When myofibroblasts were absent from the substrate (Fig. 4 *C*, *top row*), V_{REST} distribution was uniform, and the corresponding activation maps had smooth isochrones.

The substrate with only GJR in the fibrotic lesions (*2nd from right substrate* in Fig. 3) exhibited a similar trend of discontinuous wave propagation, resulting in jagged activation isochrones, and due again to slower conduction through fibrotic lesions. However, total LA activation time was 38 ms longer than in the control case. Thus, GJR in the fibrotic lesions caused a much larger degree of conduction slowing (total LA activation time increased by 12%) compared to that caused by myofibroblasts infiltration in the fibrotic lesions and their coupling to myocytes (total LA activation time increased by only 2%). Because PV ectopy in substrates with GJR resulted in conduction block, whereas those with only myofibroblasts did not, it follows that a large degree of conduction slowing (at least >5 ms) is necessary to support conduction block following PV ectopy in the LA. When lower values of GJR were tested and conduction slowing of 5 ms was not achieved, conduction block did not occur. When conduction was sufficiently slowed (i.e., in substrates with the GJR represented as described in the Methods section), the S3-induced wavefront encountered tissue that was both fully recovered (nonfibrotic regions), and in a refractory state (fibrotic lesions). Indeed, the red lines of conduction block in Fig. 2 correspond to the border of a densely fibrotic lesion (as seen in the *fibrotic lesion distribution* in Fig. 2).

Mechanism for reentry formation following conduction block in fibrotic lesions

The electrophysiological properties of the substrates in which a reentrant circuit resulted from PV ectopy, following conduction block, and degraded into sustained AF (i.e., atrial models with GJR and electrically coupled myofibroblasts in the fibrotic lesions) were compared to those of substrates that did not promote reentry despite the occurrence of conduction block (i.e., atrial models with GJR but without myofibroblasts in the fibrotic lesions) to determine the mechanisms by which myofibroblast presence and their coupling to myocytes rendered the fibrotic substrate arrhythmogenic. We investigated this by assessing the alterations in local action potential morphology (Fig. 4, *A* and *B*), as well as in organ-level electrophysiological behavior (Fig. 4, *C* and *D*).

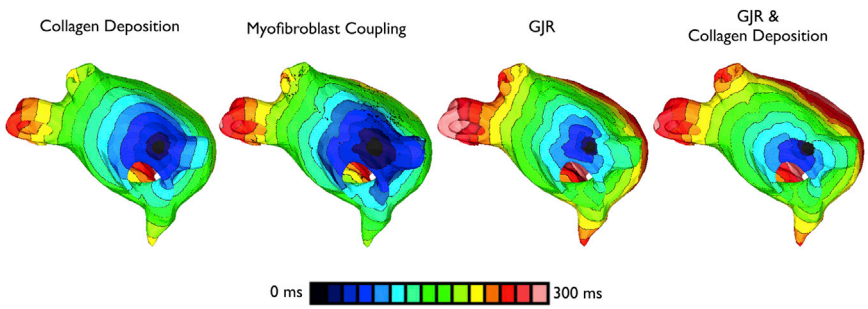

FIGURE 3 Activation maps in four atrial models, with fibrotic lesions modeled with (from *left to right*) diffuse collagen deposition, myofibroblast coupling, GJR, and the combination of GJR and diffuse collagen deposition.

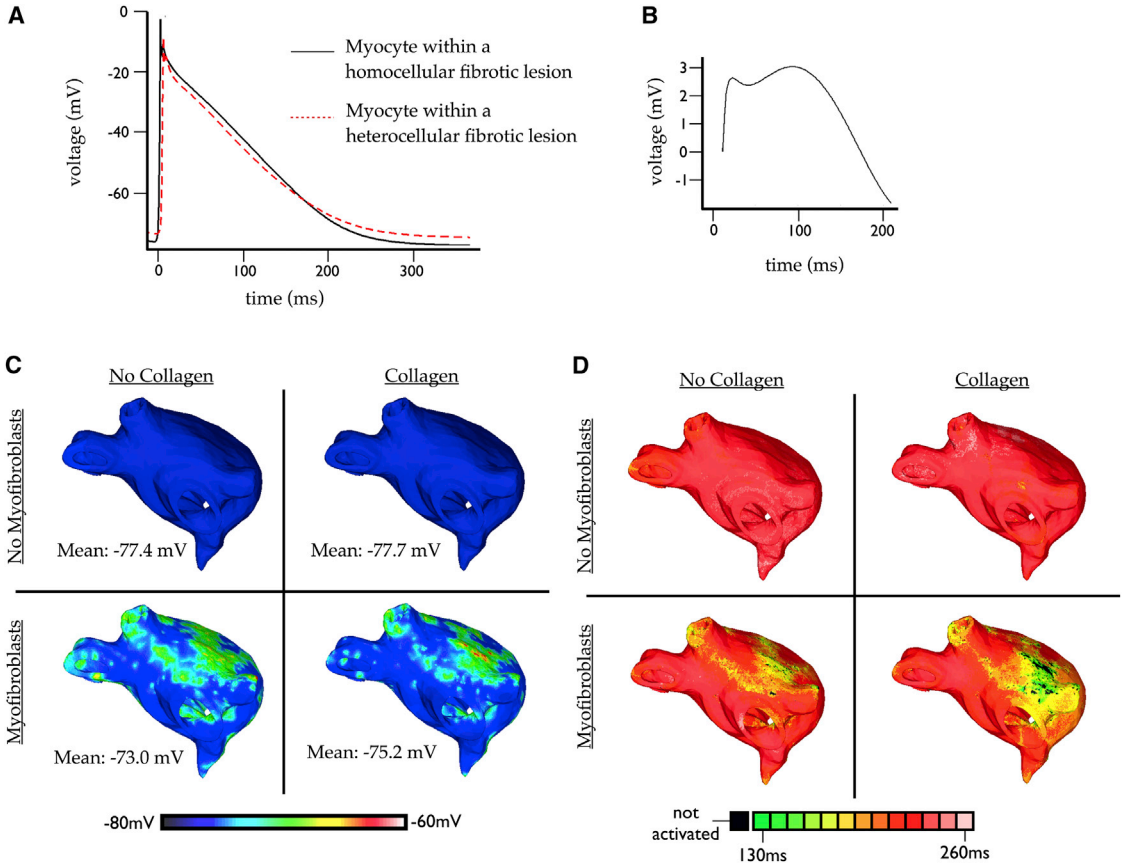

FIGURE 4 (*A*) Action potential waveforms of myocytes within homocellular (i.e., myocyte only) and heterocellular (i.e., with electrically coupled myofibroblasts and myocytes) fibrotic lesions. (*B*) Difference in transmembrane potential between the two action potential waveforms of myocytes within a fibrotic lesion (homocellular lesion myocyte – heterocellular lesion myocyte), from the action potential notch to 90% repolarization. Maps of V_{REST} (*C*) and APD (*D*) in four models. Fibrotic lesions are modeled with (*bottom row*) and without (*top row*) myofibroblast infiltration (and coupling to myocytes), as well as with (*right column*) and without (*left column*) diffuse collagen deposition for both sets of maps. All models include GJR in the fibrotic lesions.

Although myofibroblasts are inexcitable cells, they can alter action potential morphology of atrial myocytes with which they are coupled (36). Fig. 4 *A* shows how the transmembrane potential of a myocyte within a fibrotic lesion composed of an electrically connected network of myocytes and myofibroblasts (heterocellular lesion) compared to that of a myocyte within a fibrotic lesion with only other myocytes (homocellular lesion). Although the depolarization phase of the action potential remains relatively unaltered between the two waveforms, myofibroblasts exerted a clear influence on myocyte repolarization dynamics. The difference in transmembrane potential between the two waveforms (homocellular lesion myocyte – heterocellular lesion myocyte), from the action potential's notch to 90% repolarization is quantified in Fig. 4 *B*. A myocyte within a heterocellular lesion experiences reduced peak amplitude and reduced transmembrane potential at the onset of repolarization compared to a myocyte within a homocellular lesion. The degree of the transmembrane potential reduction changes over the course of repolarization, as illustrated by Fig. 4 *B*. As repolarization approaches 90%, a crossover of the action potential waveforms occur (Fig. 4 *A*), due to the elevated resting potential of the myocyte in the heterocellular lesion. At 90% repolarization, APD is shorter in myocytes within heterocellular lesions. Indeed, APD distribution at the organ level exhibits shortening in myofibroblast-infiltrated fibrotic lesions (Fig. 4 *D*, *bottom row*, and compare to Fig. 4 *D*, *top row*). Although an average APD of 219 ms was calculated across the LA without myofibroblasts in the fibrotic lesions, the average APD was 181 ms in substrates incorporating myofibroblasts in the lesions. Introducing diffuse collagen deposition into myofibroblast-infiltrated fibrotic lesions (Fig. 4 *D*, *bottom right* compared to *bottom left*) exacerbated the APD shortening caused by myofibroblasts; APD decreased to 130 ms in densely fibrotic regions. This effect is because collagen, which interrupts connections between cells, limits the distance over which myofibroblasts can exert an electrotonic influence; myofibroblasts, therefore, act as a greater local current sink when collagen is present. This also explains why collagen deposition did not alter APD in substrates without myofibroblasts (Fig. 4 *D*, *top right* compared to *top left*). The additional APD shortening caused by the inclusion of collagen deposition (diffuse or patchy) in the

fibrotic lesions was insufficient to alter the arrhythmogenic propensity of the substrates (Table 1).

Although functional coupling between myofibroblasts and myocytes is well established in the cell culture setting, direct evidence of functional gap junction formation between myofibroblasts and myocytes in the intact working myocardium is limited, having only been demonstrated in the sinoatrial node (26). However, myofibroblasts could also affect neighboring myocytes via paracrine influences. Indeed, paracrine factors released by fibroblasts have been shown to alter myocyte repolarization currents, and it has been hypothesized that these factors may contribute to the arrhythmogenic behavior of fibrotic substrates (30,37). Because the results presented herein suggest that myofibroblast-myocyte coupling alters repolarization dynamics to support reentry, we sought to determine whether direct changes in repolarization currents, as arising from paracrine effects, could also support reentrant circuit formation. Our simulation results show that atrial models in which myofibroblasts in the fibrotic lesions did not couple electrically to myocytes could also support reentry formation. This occurred when potassium currents in myocytes within the fibrotic lesions were altered. Fig. 5 presents a set of minimum paracrine alterations in the four potassium currents that was determined necessary to establish reentry formation in fibrotic models with myofibroblast proliferation but without electrical coupling to neighboring myocytes: the inward rectifier K^+ current (I_{K1}), the acetylcholine-activated K^+ current, $I_{K(ACh)}$, the rapid delayed rectifier K^+ current (I_{Kr}), and the slow delayed rectifier K^+ current (I_{Ks}). With these paracrine effects represented in the atrial model, sustained AF also ensued following PV ectopic beats; a snapshot of atrial activity encompassing multiple wavefronts is shown in Fig. 5.

DISCUSSION AND CONCLUSION

In this study, we sought to determine the mechanisms by which fibrosis and its components contribute to the degradation of PV ectopic beats into AF in the human atria. To achieve this, we used a 3D model of a patient-specific LA from a subject suffering persistent AF, capturing accurately both the atrial geometry and the distribution of fibrotic lesions. Simulations were conducted on an array of models of the same geometry/fibrosis distribution but whereby the fibrotic lesions were represented with combinations of GJR, collagen deposition, and myofibroblast proliferation, and where myofibroblasts either coupled electrically with myocytes in the fibrotic lesions or exerted equivalent paracrine influences on them. The study found that for fibrotic lesions typical of human remodeled atria under the conditions of persistent AF, the occurrence of GJR in the fibrotic lesions was a necessary but not sufficient condition for the development of AF following a PV ectopic beat. The sufficient condition was myofibroblast proliferation in these lesions, where myofibroblasts exerted either electrotonic or paracrine influences on myocytes within the lesions. Deposition of collagen in the lesions, modeled as a diffuse or patchy distribution based on experimental data, was neither a necessary nor a sufficient condition for AF development, however, it assisted the myofibroblasts' paracrine or electrotonic effects by additionally shortening APD in the lesions.

Representing the distribution of fibrotic lesions as it occurs in the human atria under the conditions of persistent AF was essential for uncovering the specific relation between atrial fibrosis and AF in the human. Atrial LGE-MRI scans from other patients with extensive enhancement exhibit similar trends in fibrotic lesion distribution (12), lacking large contiguous regions of remodeled (fibrotic) tissue—instead, the fibrotic lesions are unevenly distributed in a noncontiguous fashion throughout the LA anterior wall, posterior wall, and the atrial septum. Although reentry development in the ventricles occurs under the conditions of myocardial infarction where a large fairly contiguous region of fibrotic scar and associated peri-infarct zone both anchor the reentrant arrhythmia and determine its anatomic pathway (38), the reentrant circuits associated with AF in

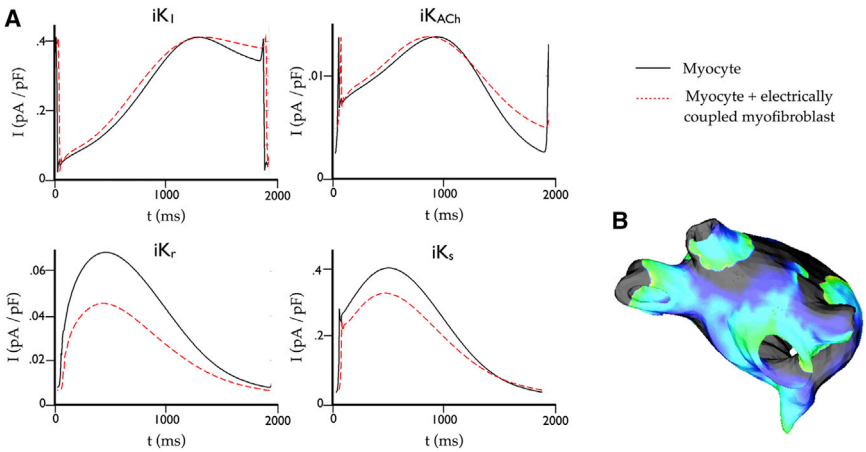

FIGURE 5 (*A*) Densities of ion currents as a function of time for a myocyte with and without an electrically coupled myofibroblast. Should paracrine effects occur, alterations in ion channel currents need to amount to these changes for reentrant circuit formation to occur without myofibroblast-to-myocyte electrical coupling. (*B*) Snapshot of AF activity in an atrial model where paracrine effects are represented in the fibrotic lesions (i.e., when potassium currents in fibrotic lesions were altered to mimic the changes that occur due to myofibroblast coupling).

the fibrotic atrium freely traverse the fibrotic regions without being anchored to any specific lesion.

This study presents a novel, to our knowledge, model of human atrial fibrosis under the conditions of persistent AF in a patient-specific representation of the atrial geometry and structure. Previous studies of fibrosis and its arrhythmogenic propensity have modeled fibrotic remodeling either by slowing conduction uniformly throughout the tissue (39) or by including only single elements of fibrosis modeled in a simplified manner, such as only fibroblasts modeled as passive resistors (40) or only collagen modeled as holes in the tissue (41). Furthermore, previous modeling efforts did not incorporate the realistic nonuniform distribution of fibrosis in the substrate (39). In contrast, our realistic model of human atrial fibrosis allows for the thorough exploration of the role of different elements of fibrotic remodeling in persistent AF.

Our finding that GJR occurrence and the resulting slowed conduction within the fibrotic lesions contributes to AF is supported by experimental evidence. When congestive heart failure, a disease strongly associated with clinical AF, was induced in dog hearts, it was found to result in discrete regions of slowed conduction and increased fibrosis compared to control (42). Furthermore, a recent study in porcine atria documented a correlation between regional Cx43 expression and sites where complex fractionated atrial electrograms (CFAE) were recorded; the expression of Cx43 at CFAE sites was significantly decreased when compared with nonCFAE sites (43).

A major finding in this study is that myofibroblast proliferation plays a key role in AF pathogenesis. Existing experimental evidence supports this finding. For one, atrial fibroblasts have a greater tendency to differentiate into activated myofibroblasts both in vitro and in vivo compared to ventricular fibroblasts (44), one explanation for why atria exhibit a more sensitive fibrotic response than ventricles in disease progression (45). Furthermore, a recent study has reported novel insights into the role of the fibroblast as the cellular link between AF and atrial fibrosis (46). In this study, it was found that transient receptor potential canonical-3 (TRPC3) channels in fibroblasts regulate cell proliferation and differentiation into myofibroblasts. The study showed that AF increases TRPC3 expression, and that TRPC3 blockade prevents AF substrate development in a dog model of electrically maintained AF, providing direct evidence of the myofibroblasts' critical role in AF. Evidence also suggests that myofibroblasts may influence the electrophysiological substrate directly through either electrical coupling with myocytes (29,47) (which has been observed in rabbit sinoatrial node (26)), or via paracrine factors (30,37). Experimental recordings from myocytes in fibroblast-conditioned media further support our findings that altered potassium currents due to myofibroblast paracrine factors may contribute to arrhythmogenesis (37).

Considerable evidence exists suggesting a correlation between AF incidence and increased collagen (5), and it has thus been hypothesized that collagen contributes to arrhythmogenesis in the fibrotic substrate. However, in a study in which Cx43 expression was similar in young and old mice, increased collagen content in adult mice was not sufficient to promote arrhythmia inducibility (48). It has also been reported that both the density and the architecture of collagen play an important role in determining its electrical influence (35). In ventricular disease progressions or in animal models in which patchy or stringy collagen may exist at higher densities, collagen was found to likely contribute to arrhythmogenesis (35). Our results did not indicate a critical role of collagen deposition in human AF initiation following PV ectopy, but that collagen deposition did not alter the arrhythmogenic outcome resulting from other fibrotic components present in the substrate, consistent with previous simulation findings (21) and with the results of a canine study of spiral wave behavior (49). It is possible that the amount of collagen correlates with AF incidence not because of its mechanistic role in arrhythmogenesis, but because increased deposition occurs as a side effect of fibroblast proliferation and differentiation, both of which may be triggered by AF itself (46), or even by GJR (50).

The insights gained in this study regarding atrial fibrosis and its relation to AF shed important light on the reasons why approaches such as Cx gene transfer (51), APD prolongation (52), and TRPC3 channel blockade (46) prevent AF in animal studies. Furthermore, by dissecting out the mechanisms by which fibrosis leads to a generation of AF following PV ectopy the study may open new doors for the development of therapeutic targets aimed at AF termination. Given the critical importance of the electrical influence of myofibroblasts in establishing an arrhythmogenic substrate, therapies that target the intercellular communication between myofibroblasts and myocytes or that block the differentiation of fibroblasts into myofibroblasts present viable upstream targets.

Limitations

The distinction between an activated fibroblast and myofibroblast is blurred throughout literature (53), and many studies concerned with one phenotype use data from the other phenotype to support their findings (54,55). The fact that fibroblasts plated under standard conditions (at low density and in serum) begin expressing the myofibroblast marker (α-SMA) within 1–2 days following isolation (56) forces us to question whether fibroblast studies in cell culture systems were, in actuality, myofibroblast studies all along (57). Although this study assumes that the myofibroblast phenotype forms under pathological conditions, it is possible that the electrical connections arising from activated fibroblasts, which may also electrically couple with myocytes or exert paracrine influences, could contribute to

arrhythmogenesis by similar mechanisms to those we propose here.

The human atrial model of fibrosis used in this study represents the atrium of one human patient with a unique distribution of fibrosis; models reconstructed from other patients would be different in both geometry and specific fibrosis distribution. However, at this point, there are practical limitations to the generation of numerous patient-specific meshes due to the high resolution of the clinical LGE-MRI scans required to create a high quality computational mesh of the human atria. As clinical MRI resolution improves, we expect that the generation of such models will become routine in the near future. However, because the fibrotic lesion size and distribution in this patient was typical for patients with extensive fibrosis in the LA and persistent AF (12), we do not expect that the conclusions regarding the roles of various components of fibrosis in arrhythmogenesis will change with different patient-specific models of the fibrotic atria.

Nonfibrotic tissue properties were modeled based on experimental findings of ion channel remodeling under AF conditions (58). However, many of the underlying pathologies that lead to persistent AF can also cause changes in ion channel properties, separate from those induced by AF (59). Further study of the effects of such changes is warranted.

SUPPORTING MATERIAL

Supporting analysis and one figure are available at http://www.biophysj.org/biophysj/supplemental/S0006-3495(13)00581-X.

The authors gratefully acknowledge support of this work by the American Heart Association Predoctoral Fellowship to K.M. and the National Institutes of Health (grants HL103428 and HL105216) to N.T. This work was supported in part by the U.S. National Science Foundation, grant NSF-OCI-108849. We also acknowledge support for image processing and model generation software from the Center for Integrative Biomedical Computing (CIBC) at the University of Utah, sponsored by NIH grant P41 GM103545-14.

REFERENCES

1. Feinberg, W. M., J. L. Blackshear, …, R. G. Hart. 1995. Prevalence, age distribution, and gender of patients with atrial fibrillation. Analysis and implications. *Arch. Intern. Med.* 155:469–473.

2. Haïssaguerre, M., P. Jaïs, …, J. Clémenty. 1998. Spontaneous initiation of atrial fibrillation by ectopic beats originating in the pulmonary veins. *N. Engl. J. Med.* 339:659–666.

3. Cappato, R., H. Calkins, …, E. Biganzoli. 2010. Updated worldwide survey on the methods, efficacy, and safety of catheter ablation for human atrial fibrillation. *Circ Arrhythm Electrophysiol.* 3:32–38.

4. Frustaci, A., C. Chimenti, …, A. Maseri. 1997. Histological substrate of atrial biopsies in patients with lone atrial fibrillation. *Circulation.* 96:1180–1184.

5. Xu, J., G. Cui, …, L. Sen. 2004. Atrial extracellular matrix remodeling and the maintenance of atrial fibrillation. *Circulation.* 109:363–368.

6. Mariscalco, G., K. G. Engström, …, A. Sala. 2006. Relationship between atrial histopathology and atrial fibrillation after coronary bypass surgery. *J. Thorac. Cardiovasc. Surg.* 131:1364–1372.

7. Mahnkopf, C., T. J. Badger, …, N. F. Marrouche. 2010. Evaluation of the left atrial substrate in patients with lone atrial fibrillation using delayed-enhanced MRI: implications for disease progression and response to catheter ablation. *Heart Rhythm.* 7:1475–1481.

8. Kostin, S., G. Klein, …, J. Schaper. 2002. Structural correlate of atrial fibrillation in human patients. *Cardiovasc. Res.* 54:361–379.

9. Rohr, S. 2009. Myofibroblasts in diseased hearts: new players in cardiac arrhythmias? *Heart Rhythm.* 6:848–856.

10. Akoum, N., M. Daccarett, …, N. Marrouche. 2011. Atrial fibrosis helps select the appropriate patient and strategy in catheter ablation of atrial fibrillation: a DE-MRI guided approach. *J. Cardiovasc. Electrophysiol.* 22:16–22.

11. McDowell, K. S., F. Vadakkumpadan, …, N. A. Trayanova. 2012. Methodology for patient-specific modeling of atrial fibrosis as a substrate for atrial fibrillation. *J. Electrocardiol.* 45:640–645.

12. Oakes, R. S., T. J. Badger, …, N. F. Marrouche. 2009. Detection and quantification of left atrial structural remodeling with delayed-enhancement magnetic resonance imaging in patients with atrial fibrillation. *Circulation.* 119:1758–1767.

13. Narayan, S. M., D. E. Krummen, …, J. M. Miller. 2012. Treatment of atrial fibrillation by the ablation of localized sources: confirm (conventional ablation for atrial fibrillation with or without focal impulse and rotor modulation) trial. *J. Am. Coll. Cardiol.* 60:628–636.

14. Vadakkumpadan, F., H. Arevalo, …, N. Trayanova. 2012. Image-based estimation of ventricular fiber orientations for personalized modeling of cardiac electrophysiology. *IEEE Trans. Med. Imaging.* 31:1051–1060.

15. Courtemanche, M., R. J. Ramirez, and S. Nattel. 1999. Ionic targets for drug therapy and atrial fibrillation-induced electrical remodeling: insights from a mathematical model. *Cardiovasc. Res.* 42:477–489.

16. Krummen, D. E., J. D. Bayer, …, S. M. Narayan. 2012. Mechanisms of human atrial fibrillation initiation: clinical and computational studies of repolarization restitution and activation latency. *Circ Arrhythm Electrophysiol.* 5:1149–1159.

17. Kneller, J., R. Q. Zou, …, S. Nattel. 2002. Cholinergic atrial fibrillation in a computer model of a two-dimensional sheet of canine atrial cells with realistic ionic properties. *Circ. Res.* 90:E73–E87.

18. Hansson, A., M. Holm, …, S. B. Olsson. 1998. Right atrial free wall conduction velocity and degree of anisotropy in patients with stable sinus rhythm studied during open heart surgery. *Eur. Heart J.* 19:293–300.

19. Costa, C. M., F. O. Campos, …, G. Plank. 2011. A finite element approach for modeling micro-structural discontinuities in the heart. *Conf. Proc. IEEE Eng. Med. Biol. Soc.* 2011:437–440.

20. Boldt, A., U. Wetzel, …, S. Dhein. 2004. Fibrosis in left atrial tissue of patients with atrial fibrillation with and without underlying mitral valve disease. *Heart.* 90:400–405.

21. Ashihara, T., R. Haraguchi, …, N. A. Trayanova. 2012. The role of fibroblasts in complex fractionated electrograms during persistent/permanent atrial fibrillation: implications for electrogram-based catheter ablation. *Circ. Res.* 110:275–284.

22. Turner, I., C. L-H Huang, and R. C. Saumarez. 2005. Numerical simulation of paced electrogram fractionation: relating clinical observations to changes in fibrosis and action potential duration. *J. Cardiovasc. Electrophysiol.* 16:151–161.

23. Lellouche, N., E. Buch, …, K. Shivkumar. 2007. Functional characterization of atrial electrograms in sinus rhythm delineates sites of parasympathetic innervation in patients with paroxysmal atrial fibrillation. *J. Am. Coll. Cardiol.* 50:1324–1331.

24. Luo, M. H., Y. S. Li, and K. P. Yang. 2007. Fibrosis of collagen I and remodeling of connexin 43 in atrial myocardium of patients with atrial fibrillation. *Cardiology.* 107:248–253.

25. Du, J., J. Xie, …, L. Yue. 2010. TRPM7-mediated Ca2+ signals confer fibrogenesis in human atrial fibrillation. *Circ. Res.* 106:992–1003.

26. Camelliti, P., C. R. Green, …, P. Kohl. 2004. Fibroblast network in rabbit sinoatrial node: structural and functional identification of homogeneous and heterogeneous cell coupling. *Circ. Res.* 94:828–835.

27. McDowell, K. S., H. J. Arevalo, …, N. A. Trayanova. 2011. Susceptibility to arrhythmia in the infarcted heart depends on myofibroblast density. *Biophys. J.* 101:1307–1315.

28. Vigmond, E. J., M. Hughes, …, L. J. Leon. 2003. Computational tools for modeling electrical activity in cardiac tissue. *J. Electrocardiol.* 36(*Suppl*):69–74.

29. Miragoli, M., G. Gaudesius, and S. Rohr. 2006. Electrotonic modulation of cardiac impulse conduction by myofibroblasts. *Circ. Res.* 98:801–810.

30. Vasquez, C., P. Mohandas, …, G. E. Morley. 2010. Enhanced fibroblast-myocyte interactions in response to cardiac injury. *Circ. Res.* 107:1011–1020.

31. Kuo, C. S., K. Munakata, …, B. Surawicz. 1983. Characteristics and possible mechanism of ventricular arrhythmia dependent on the dispersion of action potential durations. *Circulation.* 67:1356–1367.

32. Weber, F. M., A. Luik, …, O. Dossel. 2011. Conduction velocity restitution of the human atrium–an efficient measurement protocol for clinical electrophysiological studies. *IEEE Trans. Biomed. Eng.* 58:2648–2655.

33. Lalani, G. G., A. Schricker, …, S. M. Narayan. 2012. Atrial conduction slows immediately before the onset of human atrial fibrillation: a bi-atrial contact mapping study of transitions to atrial fibrillation. *J. Am. Coll. Cardiol.* 59:595–606.

34. Spach, M. S., J. F. Heidlage, …, R. C. Barr. 2007. Mechanism of origin of conduction disturbances in aging human atrial bundles: experimental and model study. *Heart Rhythm.* 4:175–185.

35. Kawara, T., R. Derksen, …, J. M. de Bakker. 2001. Activation delay after premature stimulation in chronically diseased human myocardium relates to the architecture of interstitial fibrosis. *Circulation.* 104:3069–3075.

36. Maleckar, M. M., J. L. Greenstein, …, N. A. Trayanova. 2009. Electrotonic coupling between human atrial myocytes and fibroblasts alters myocyte excitability and repolarization. *Biophys. J.* 97:2179–2190.

37. Pedrotty, D. M., R. Y. Klinger, …, N. Bursac. 2009. Cardiac fibroblast paracrine factors alter impulse conduction and ion channel expression of neonatal rat cardiomyocytes. *Cardiovasc. Res.* 83:688–697.

38. Verma, A., N. F. Marrouche, …, A. Natale. 2005. Relationship between successful ablation sites and the scar border zone defined by substrate mapping for ventricular tachycardia post-myocardial infarction. *J. Cardiovasc. Electrophysiol.* 16:465–471.

39. Krogh-Madsen, T., G. W. Abbott, and D. J. Christini. 2012. Effects of electrical and structural remodeling on atrial fibrillation maintenance: a simulation study. *PLOS Comput. Biol.* 8:e1002390.

40. Wolf, R. M., P. Glynn, …, T. J. Hund. 2013. Atrial fibrillation and sinus node dysfunction in human ankyrin-B syndrome: a computational analysis. *Am. J. Physiol. Heart Circ. Physiol.* 304:H1253–H1266.

41. Burstein, B., P. Comtois, …, S. Nattel. 2009. Changes in connexin expression and the atrial fibrillation substrate in congestive heart failure. *Circ. Res.* 105:1213–1222.

42. Li, D., S. Fareh, …, S. Nattel. 1999. Promotion of atrial fibrillation by heart failure in dogs: atrial remodeling of a different sort. *Circulation.* 100:87–95.

43. Liu, X., H. F. Shi, …, J. N. Gu. 2009. Decreased connexin 43 and increased fibrosis in atrial regions susceptible to complex fractionated atrial electrograms. *Cardiology.* 114:22–29.

44. Burstein, B., E. Libby, …, S. Nattel. 2008. Differential behaviors of atrial versus ventricular fibroblasts: a potential role for platelet-derived growth factor in atrial-ventricular remodeling differences. *Circulation.* 117:1630–1641.

45. Hanna, N., S. Cardin, …, S. Nattel. 2004. Differences in atrial versus ventricular remodeling in dogs with ventricular tachypacing-induced congestive heart failure. *Cardiovasc. Res.* 63:236–244.

46. Harada, M., X. Luo, …, S. Nattel. 2012. Transient receptor potential canonical-3 channel-dependent fibroblast regulation in atrial fibrillation. *Circulation.* 126:2051–2064.

47. Gaudesius, G., M. Miragoli, …, S. Rohr. 2003. Coupling of cardiac electrical activity over extended distances by fibroblasts of cardiac origin. *Circ. Res.* 93:421–428.

48. van Veen, T. A., M. Stein, …, H. V. van Rijen. 2005. Impaired impulse propagation in Scn5a-knockout mice: combined contribution of excitability, connexin expression, and tissue architecture in relation to aging. *Circulation.* 112:1927–1935.

49. Ikeda, T., M. Yashima, …, H. S. Karagueuzian. 1997. Attachment of meandering reentrant wave fronts to anatomic obstacles in the atrium. Role of the obstacle size. *Circ. Res.* 81:753–764.

50. Jansen, J. A., T. A. van Veen, …, H. V. van Rijen. 2012. Reduced Cx43 expression triggers increased fibrosis due to enhanced fibroblast activity. *Circ Arrhythm Electrophysiol.* 5:380–390.

51. Igarashi, T., J. E. Finet, …, J. K. Donahue. 2012. Connexin gene transfer preserves conduction velocity and prevents atrial fibrillation. *Circulation.* 125:216–225.

52. Amit, G., K. Kikuchi, …, J. K. Donahue. 2010. Selective molecular potassium channel blockade prevents atrial fibrillation. *Circulation.* 121:2263–2270.

53. Camelliti, P., T. K. Borg, and P. Kohl. 2005. Structural and functional characterization of cardiac fibroblasts. *Cardiovasc. Res.* 65:40–51.

54. Zlochiver, S., V. Muñoz, …, J. Jalife. 2008. Electrotonic myofibroblast-to-myocyte coupling increases propensity to reentrant arrhythmias in two-dimensional cardiac monolayers. *Biophys. J.* 95:4469–4480.

55. MacCannell, K. A., H. Bazzazi, …, W. R. Giles. 2007. A mathematical model of electrotonic interactions between ventricular myocytes and fibroblasts. *Biophys. J.* 92:4121–4132.

56. Wang, J., H. Chen, …, C. A. McCulloch. 2003. Mechanical force regulation of myofibroblast differentiation in cardiac fibroblasts. *Am. J. Physiol. Heart Circ. Physiol.* 285:H1871–H1881.

57. Rohr, S. 2011. Cardiac fibroblasts in cell culture systems: myofibroblasts all along? *J. Cardiovasc. Pharmacol.* 57:389–399.

58. Courtemanche, M., R. J. Ramirez, and S. Nattel. 1998. Ionic mechanisms underlying human atrial action potential properties: insights from a mathematical model. *Am. J. Physiol.* 275:H301–H321.

59. Cha, T. J., J. R. Ehrlich, …, S. Nattel. 2004. Atrial ionic remodeling induced by atrial tachycardia in the presence of congestive heart failure. *Circulation.* 110:1520–1526.